Hindawi
Cellular Microbiology
Volume 2023, Article ID 7369034, 16 pages
https://doi.org/10.1155/2023/7369034

Research Article

Liver Microbiome in Healthy Rats: The Hidden Inhabitants of Hepatocytes

Xiao Wei Sun, Hua Zhang, Xiao Zhang, Peng Fei Xin, Xue Gao, Hong Rui Li, Cai Yun Zhou, Wen Min Gao, Xuan Xuan Kou, and Jian Gang Zhang

Pathology Institute, School of Basic Medical Sciences, Lanzhou University, Lanzhou 730000, China

Correspondence should be addressed to Xiao Wei Sun; sunxw@lzu.edu.cn and Jian Gang Zhang; zhjg@lzu.edu.cn

Received 30 August 2022; Revised 7 January 2023; Accepted 19 January 2023; Published 31 January 2023

Academic Editor: Shiek Ahmed

The tumor and tissue microbiota of human beings have recently been investigated. Gut permeability is known as a possible resource for the positive detection of tissue bacteria. Herein, we report that microbiota were detected in high abundance in the hepatocytes of healthy rats and that they were shared with the gut microbiota to an extent. We assessed male Sprague Dawley (SD) rats for the 16S ribosomal ribonucleic acid (rRNA) gene. After the rats were sacrificed by blood drainage from the portal vein, we extracted total deoxyribonucleic acid (DNA) from their ileal and colonic contents and liver tissues. The V3–V4 region of the 16S rRNA gene was amplified by polymerase chain reaction (PCR) and sequenced using an Illumina HiSeq 2500 platform. Sequences were assigned taxonomically by the SILVA database. We also detected bacterial lipopolysaccharide (LPS) and lipoteichoic acid (LTA) in situ using immunofluorescence (IF) and western blotting and the 16S rRNA gene using fluorescent in situ hybridization (FISH). In the livers of six rats, we detected $54{,}867.50 \pm 6450.03$ effective tags of the 16S rRNA gene and clustered them into 1003 kinds of operational taxonomic units (OTUs; 805.67 ± 70.14, 729–893). Rats showed conservation of bacterial richness, abundance, and evenness. LPS and the 16S rRNA gene were detected in the nuclei of hepatocytes. The main function composition of the genomes of annotated bacteria was correlated with metabolism ($79.92 \pm 0.24\%$). Gram negativity was about 1.6 times higher than gram positivity. The liver microbiome was shared with both the small and large intestines but showed significantly higher richness and evenness than the gut microbiome, and the β-diversity results showed that the liver microbiome exhibited significantly higher similarity than the small and large intestines ($P < 0.05$). Our results suggest that the bacteria in the liver microbiome are hidden intracellular inhabitants in healthy rat livers.

1. Introduction

With the help of high-throughput nucleotide sequencing and using the 16S ribosomal ribonucleic acid (rRNA) gene as a highly conserved marker in bacterial clades, gut microbiota—which are distributed throughout the whole gastrointestinal (GI) tract with diverse microbial communities—could be identified [1].

By collecting feces and analyzing the intestinal microbiota composition and its metabolites in health and disease, many human sample population studies have further proven the relationship between gut microbiome (mainly fecal microbiome) alterations and the occurrence of various diseases [2–6]. These studies and reviews strongly suggested the gut microbiota mechanism of diseases [7, 8].

Recently, researchers have found that a high-fat diet can elevate gut permeability and result in bacterial translocation from the intestine into tissues such as adipose and liver tissues [9–12]. In our recent study, we also found that in feeding after-fasting or obesity rats, the villi of the small intestine formed a channel, providing transient and functional unrestricted channel absorption (data not shown). These results clearly indicated that gut leakage was the pathway by which gut microbiota resulted in diseases [13].

In addition, studies have also demonstrated bacteria in various tumor cells and proposed the concept of tumor type-specific intracellular bacteria [14]. Moreover, several studies have suggested the existence of tissue microbiota either in humans or in mice [15–18]. The 16S rRNA gene signature was also demonstrated in the blood of healthy

humans (primarily leukocyte and platelet fractions) [19] or patients [20, 21] as well as in the circulation of animals [22–24]. These key factors illustrate the crosstalk line between the gut microbiota, circulation, and tissues [25]; that is, the gut microbiota enter into the circulation through leakage and locate into tissues and change into tissue microbiota/tumor type-specific intracellular bacteria. They then cause disease, although the mechanism of tissue microbiota development remains a hypothesis [26].

Based on this route, the liver is inevitably the frontier organ (the key gatekeeper) through which the gut microbiota enters into circulation. This relationship can be described as the "gut-liver axis" [27]. The results of a study by Sookoian et al. support this possibility. Bacterial DNA was detected in nonalcoholic fatty liver disease (NAFLD) in obesity patients, and the LPS was detected in the portal tract by immunohistochemistry [26]. It can also be deduced that the liver, as well as the mesenteric lymph nodes, plays immune filtering functions similar to the spleen and exports bacteria to the circulation as the transfer station. Regarding the complicated pathogenesis of diseases in visceral organs that are independent of gut and liver impairment, it is of great significance to investigate the liver bacteria in healthy individuals and clarify the relationship with the gut microbiota.

The objective of this study was to confirm the existence of the liver microbiome, its composition and location characteristics, and its relevance to the gut microbiome. The rationale of the study is as follows: (1) microbiota were detected with high-throughput 16S rRNA gene sequencing [1]; (2) the location of liver microbiota was confirmed by detecting LPS, LTA, or 16S rRNA gene in situ using immunofluorescence (IF) [14], fluorescence *in situ* hybridization (FISH), and western blotting; and (3) the liver and gut microbiome relevance was confirmed by comparing their composition and diversity. Herein, we reported bacteria in the normal liver tissues and hepatocytes of rats without dietary interference or disease development. The comparison between the liver and gut microbiota suggests an inherent inhabitant of the liver microbiome in hepatocytes, and the "liver to gut" crosstalk of the microbiota can be deduced.

2. Materials and Methods

2.1. Animals. Male adult Sprague-Dawley (SD) rats, 22 weeks old with a body weight of 270–360 g (ordinary rats) or 8 weeks old with a body weight of 250–280 g (clean rats), were used for 16S rRNA gene sequencing or location detection. All animals received humane care, and the study protocols, complied with the Laboratory Animal—Guideline for Ethical Review of Animal Welfare (GB/T 35892—2018) and were approved by the Medical Ethics Committee of Lanzhou University (jcyxy20190302). This study also conformed to the Animal Research: Reporting of In Vivo Experiments (ARRIVE) guidelines and Replacement, Refinement and Reduction of Animals in Research (NC3Rs).

2.2. Sample Collection and Contamination Avoidance. Animals were anesthetized with pentobarbital sodium (5 mg/100 g body mass) to avoid their suffering at each stage of the experiment, followed by three skin sterilizations using 75% ethanol and iodophor. To avoid environmental contamination, all operations were conducted under a laminar flow hood following aseptic surgery protocols, including the use of a surgical towel, and avoided contact between the skin and subcutaneous tissue. After the skin was opened, we discarded the original set of all surgical instruments and used another set. To eliminate possible blood contamination, animals were sacrificed by portal vein blood drainage. To prevent possible fecal contamination, we began by removing liver tissues, then those of the ileum (small intestine (SI)) and colon (large intestine (LI)). Subsequently, SI and LI contents were pushed out from the outside of the gut using another set of tweezers. Livers were separated and sampled without perfusion. All samples were collected in DNA-free clean Eppendorf Tubes and stored at −80°C after a quick freeze in liquid nitrogen. To avoid possible contamination during 16S rRNA gene analysis, we transported samples on dry ice to a sequencing company (BMK Co., Beijing, China), which provided an integrated service in DNA extraction, polymerase chain reaction (PCR) amplification, and sequencing via procedures that strictly avoided contamination.

2.3. Bacterial DNA Extraction. We extracted total DNA from frozen liver and fecal samples (0.25–0.5 g) using a Magnetic Soil and Stool DNA Kit (#DP812; TianGen Corp., Beijing, China, https://www.tiangen.com/) per the kit protocol. All procedures were performed with sterile and disposable materials to avoid cross-contamination; in addition, beads and DNA extraction blank controls were used during this process. The volume of total DNA solution was 40.0 μl with OD_{260}/OD_{280} values of 1.86–1.97, and the nanodrop concentration ranged from 42.2–176.3 ng/μl. For the few sample concentrations lower than 5 ng/μl and with OD_{260}/OD_{280} exceeding the detecting range of the instruments (i.e., out of the range of 1.8–2.0), we determined bacterial DNA, as well as its integrity, with preamplified PCR products using 1.8% agar gel. Briefly, the 16S rRNA gene's variable region 3–4 (V3–V4) was amplified using PCR (1 μl original solution, Q enzyme, 30 cycles), and the products were checked using 1.8% agar gel (120 V, 40 min). Then, we qualified them by analyzing the gel images via ImageJ software (National Institutes of Health, Bethesda, MD, USA). The positive bands proved the existence of bacterial DNA in samples, meeting the criteria for further sequencing.

2.4. 16S PCR and Sequencing Library Construction. We used two-round-tailed PCR with the barcode at the end of the primer for 16S amplification and sequencing. In the first round, the 16S rRNA gene's V3–V4 region was amplified with an initial heating step of 95°C for 5 min, followed by 25 cycles of 30 s at 95°C, 30 s at 50°C, 40 s at 72°C, and a final extension step of 72°C for 7 min. The bacterial primer was as follows: 338F: 5′-ACTCCTACGGGAGGCAGCA-3′; 806R: 5′-GGACTACHVGGGTWTCTAAT-3′ [28]. The reaction system was as follows: bacterial genome DNA, 50.0 ng ± 20%; primers (338F and 806R, 10 μM; Synbio Technologies, Suzhou, China), 0.3 μl each; KOD FX Neo Buffer (KFX-201S;

TOYOBO; Biolink Biotechnology, Beijing, China, http://www.bjbiolink.com/), 5.0 μl; deoxyribose nucleotide triphosphate (dNTP; 2 mM each), 2.0 μl; KOD FX Neo, 0.2 μl; and double-distilled water (ddH_2O) added to 10.0 μl. We established a negative control and used sterile water instead of DNA for PCR amplification. We performed the PCR reaction using an Applied Biosystems PCR System (Veriti 96-Well 9902; Applied Biosystems, Foster City, CA, USA). PCR products (10-μl system) were purified using VAHTSTM DNA clean beads (Vazyme Corp., Nanjing, China, http://www.vazyme.com/) at a ratio of 1 : 1, and eluted using 8.0–10.0 μl ddH_2O. In the second round of PCR reaction (Solexa PCR), dual-indexed sequences (barcodes) and Illumina adaptors (Illumina, Inc., San Diego, CA, USA) were added to the amplicon. The reaction system was as follows: purified V3–V4 PCR production DNA, 5.0 μl; primers (MPPI-a and MPPI-b, 2.0 μM; Synbio Technologies, Suzhou, China), 2.5 μl each; NEBNext® Ultra™ II Q5® Master Mix (New England Biolabs, Ipswich, MA, USA) (M0544L; Biolink Biotechnology, Beijing, China) 10.0 μl. The PCR reaction was performed at 98°C for 30 s, with 10 cycles of 98°C for 10 s, 65°C for 30 s, 72°C for 30 s, and an extension at 72°C for 5 min.

We detected the products using 1.8% agar gel and qualified them by analyzing the gel images via Image J software. Next, we mixed 150 ng of each sample (samples were 1.5–14.0 μl) and purified it using an E.Z.N.A. Cycle-Pure Kit (Omega Bio-Tek, Inc., Norcross, GA, USA). The products were recovered using Monarch DNA Gel Extraction (NEB, T1020L) in 1.8% agar gel.

2.5. Sequencing. After quality testing on a Qsep-400 (BiOptic, Inc., New Taipei City, Taiwan, ROC) and preparation of a flow cell chip, we subjected 500 ng PCR products to paired-end (PE) sequenced on an Illumina HiSeq 2500 platform (Illumina, Inc., San Diego, CA, USA) at Biomarker Technologies Co, Ltd. (Beijing, China) according to standard protocols. The sequencing length was 350–450 bp. Original image data files were transformed into raw data (PE reads) via base calling analysis. The negative control was not sequenced because it was bandless and sequencing would have been meaningless.

2.6. Quality Assessment and Data Processing. According to the overlapping relationship, PE reads were merged with Fast Length Adjustment of SHort reads (FLASH) software v.1.2.7 (Johns Hopkins University Center for Computational Biology, Baltimore, MD, USA; raw tags) [29]. We discarded tags with >6 mismatches. The minimum overlap length was 10 bp, and the maximum mismatch ratio allowed in the overlap region was 0.2 (default). Raw tags with an average quality score < 20 in a 50 bp sliding window were then filtered using Trimmomatic software v.0.33 (http://USADELLAB.org) [30] and those shorter than 350 bp were removed (clean tags). We further removed possible chimeras using UCHIME v.4.2 (http://drive5.com/usearch/manual/uchime_algo.html) [31] to obtain effective tags.

2.7. Operational Taxonomic Unit Analysis. Effective tags were clustered at a 97% similarity level to obtain OTUs using USEARCH software v.10.0 [32]. We evaluated the α-diversity index of each sample using mothur software v.1.30 (http://mothur.org/) and the β-diversity index using Quantitative Insights Into Microbial Ecology (QIIME) software v2.2. Degrees of similarity in species diversity between different samples were compared.

2.8. Taxonomic Analysis. We compared representative OTU sequences against the SILVA microbial reference database (release 128; http://www.arb-silva.de) [33]. The classification information of each OTU was obtained by comparison, and the OTU was annotated using RDP Classifier (v2.2; QIIME) [34]. Next, we counted the community composition of each sample at phylum, class, order, family, genus, and species levels. Species richness at different taxonomic levels was assessed using QIIME, and the community structure diagram of each taxonomic level was drawn using R software v3.1.1 (R Foundation for Statistical Computing, Vienna, Austria).

2.9. Immunofluorescence Assays. Immunofluorescence (IF) staining was performed according to standard staining methods as described, with slight modifications [9]. Briefly, we fixed frozen liver tissue sections (4 μm) with 4% paraformaldehyde for 30 min and aged them at 60°C for 10 min, followed by incubation with 0.3% Triton X-100 (#T8200; Solarbio) and 3% bovine serum albumin (BSA; B2064-50G; Sigma Germany, Munich, Germany) for 30 min. A blank slide without a sample was set. Primary antibodies (lipopolysaccharide (LPS) core monoclonal antibody [mAb] WN1 222-5, #HM6011, 1 : 400 dilution; lipoteichoic acid (LTA), mAb 55, #HM2048; 1 : 400 dilution; both from Hycult Biotech, Uden, Netherlands) or phosphate-buffered saline (PBS; #BL601A; Biosharp Life Sciences, Hefei, China) as the negative control were applied to slides overnight at 4°C; secondary antibody (DyLight 488 goat anti-mouse immunoglobulin G [IgG]; Ex/Em = 493/518 nm, #AMJ-AB2004; 1 : 800 dilution; AmyJet Scientific Inc., Wuhan, China) were added for 1 h at 37°C. We counterstained the slides with 4′,6-diamidino-2-phenylindole (DAPI; 0.5 μg/ml; Ex/Em =364/454, #BL105A; Biosharp) at room temperature (RT) for 10 min, and then dried the slices in a dark room and mounted them with an anti-fluorescence attenuator mountant. Paraformaldehyde fixed *Staphylococcus* (Newman strain) and *Escherichia coli* (MG1655 strain) (preserved and kind gifts from Professor Jian Han (Lan Zhou University, China) were used as Gram-positive and Gram-negative controls, respectively. We observed and recorded slides using Nikon-ECLIPSE 80i/DS-Ri2/NIS-Element D microscopy (Nikon, Tokyo, Japan).

2.10. Equipment and Settings. Images were captured using the software NIS-Element D using a Nikon-ECLIPSE 80i upright fluorescence microscope outfitted with a Nikon DS-Ri2 camera, Plan Fluor 40x DIC M N2 objective (objective numerical aperture: 0.75, refractive index: 1.000). The images were acquired at 96 dpi in the x- and y-axis with pixel dimensions of 4908 × 3264, and the image bit depth was 24.

2.11. 16S rRNA Fluorescent In Situ Hybridization. We detected the 16S rRNA in tissues according to the instructions of a EUB338 FISH Probe Kit (#20 μM; FBPC-10;

Creative Bioarray, Shirley, NY, USA). Briefly, frozen tissue slides (4 μm) were fixed with 4% paraformaldehyde for 30 min and at 60°C for 10 min, followed by incubation with 0.3% Triton X-100 for 30 min. We then incubated the slides in lysozyme at 37°C for 15 min. As a positive control, a bacteria smear was incubated in 0.01 M HCl at RT for 20 min. Slides were fixed with 4% paraformaldehyde for another 15 min at RT, after which we treated them with diethyl pyrocarbonate (DEPC) for 10 min and incubated them with BSA (3%) for 2 h. BSA was then discarded, and fluorescein isothiocyanate (FITC)-labeled probes (EUB338 GCTGCC TCCCGTAGGAGT) and a nonspecific complement probe (nEUB338 CGACGGAGGG CATCCTCA; #FBPC-13; Creative Bioarray) were hybridized in a pre-warmed humidified hybridization chamber and incubated overnight at 39°C (range, 38–42°C). We diluted FISH probe EUB338 or nEUB338 with 35% hybridization buffer (1 : 100), denatured it at 84°C for 5 min, and then incubated at 37°C for 3 min. After hybridization, we carefully removed the sealing film by soaking the slides in wash solution (WS; 2 × saline-sodium citrate [SSC]/0.1% Tween 20) at RT for 15 min to loosen the coverslips. Slides were then rinsed twice in WS for 15 min each time, immersed in 75% and 100% ethanol for 2 min, and then air-dried for 20 min. We counterstained the slides with DAPI antifade solution (using EUB338 FISH Probe Kit) for 10 min and examined them under the Nikon fluorescence microscope.

2.12. LPS and LTA Western Blotting. We separated cytoplasmic from nuclear components using a Minute™ Cytoplasmic and Nuclear Fractionation Kit for Cells (#sc-003; Invent, Beijing, China). The liver tissue was washed with precooled sterile PBS, and 60 mg of fresh (or frozen) soft liver tissue was added to a 1.5 ml sterile microcentrifuge tube. We then added 200 μl of precooled sterile PBS to the same tube and ground the tissue with a clean plastic grinding rod for 2–3 min on ice until no solid tissue was visible, after which the frozen liver tissue sample was thawed completely on ice and then ground again. After incubation on ice for 5 min, we carefully transferred the supernatant into another precooled sterile 1.5 ml microcentrifuge tube. Cells were harvested from the suspension by low-speed centrifugation (500 × g) at 4°C for 3 min. We added 200 μl cytoplasmic extraction buffer for every 20 μl of cell volume, vortexed the tube vigorously for 15 s, and incubated it on ice for 15 min. Then, we centrifuged it for 5 min at 16000 × g and 4°C in a microcentrifuge. The supernatant (cytosol fraction) was transferred to a fresh prechilled 1.5 ml tube; the pellet was washed in 0.5 ml cold PBS, centrifuged at 8000 × g for 5 min to reduce contamination of cytosolic proteins and frozen at −80°C. We added 100 μl nuclear extraction buffer to the pellet (ratio of cytoplasmic to nuclear extraction buffer, 2 : 1), vortexed the mixture vigorously for 30 s, and incubated the tube on ice for 2 min; this sequence of steps was repeated five times. Immediately afterward, we transferred the nuclear extract to a prechilled filter cartridge via a collection tube and centrifuged it at 16000 × g in the microcentrifuge for 30 s at 4°C. We discarded the filter cartridge and stored the nuclear extract at −80°C. Measurements were repeated three times for every sample, and blanks without liver samples were established. The bicinchoninic acid (BCA) method was used to measure protein concentrations. Protein samples were separated by sodium dodecyl sulfate polyacrylamide gel electrophoresis (SDS-PAGE; 12% separating gel), transferred onto a polyvinylidene difluoride (PVDF) membrane (Millipore Sigma, Burlington, MA, USA), and probed with the above-indicated primary antibodies at 4°C overnight, followed by the appropriate secondary horseradish peroxide (HRP)-conjugated IgG antibody at RT for 1 h. The following antibodies were used: primary, LPS (1 : 400; HM6011; Hycult), LTA (1 : 1000; #HM2048; Hycult), Lamin-B1 (1 : 2000, #ab16048; Abcam, Cambridge, UK), glyceraldehyde 3-phosphate dehydrogenase (GAPDH; 1 : 4000; #YM3215; Proteintech, Chicago, IL, USA); secondary, HRP-labeled goat anti-rabbit (1 : 5000, #RS0002; ImmunoWay Biotechnology Co., Plano, TX, USA) and HRP-labeled goat anti-mouse (1 : 5000; #RS0001; ImmunoWay). Protein bands were visualized using an electrochemiluminescence (ECL) kit (Super ECL Detection Reagent, Yeasen Biotechnology Co., Ltd., Shanghai, China) and ImageJ software v6.0.

Table 1: Alpha diversity among individual liver samples.

Sample	Ace	Chao	Shannon	Simpson
A5	920.47	936.60	8.02	0.99
A12	737.07	735.90	7.94	0.99
A29	906.05	921.79	8.08	0.99
A32	868.85	878.24	8.03	0.99
A36	797.98	810.00	8.06	0.99
A46	749.48	760.69	7.90	0.99
CV	0.096	0.100	0.009	0.001

CV: coefficient of variation, calculated as standard deviation (SD) divided by mean. Simpson index was calculated as $1 - \sum pi^2$.

2.13. Statistical Analysis. All data were expressed as mean ± standard deviation. We conducted all statistical analyses using SPSS software v19.0 (IBM Corp., Armonk, NY, USA). The Kruskal-Wallis H rank test was used for comparisons between the liver, SI, and LI samples, and a one-way analysis of variance (ANOVA) was used for mean comparison of the distance between the liver, SI, and LI samples. Differences were considered statistically significant at $P < 0.05$.

3. Results

3.1. Liver Microbiota Detected by 16S rRNA Gene Sequencing. We sequenced the V3–V4 region of the 16S rRNA gene in liver tissues, obtaining 54,867.50 ± 6,450.03 effective tags (Table S1). These tags were further clustered into 1003 kinds of OTUs (805.67 ± 70.14, 729–893), of which six rats shared 598 kinds of OTUs. Annotated species numbers at different levels are summarized in Table S2. Individuals showed obvious conservation of bacterial abundance (tags), richness (OTU number), and evenness (Table 1). The coefficient of variation (CV) of the α-diversity index was low.

At the phylum level, liver microbiota were annotated and clustered into 19 species. No exclusive species was observed among individuals. Firmicutes, Proteobacteria,

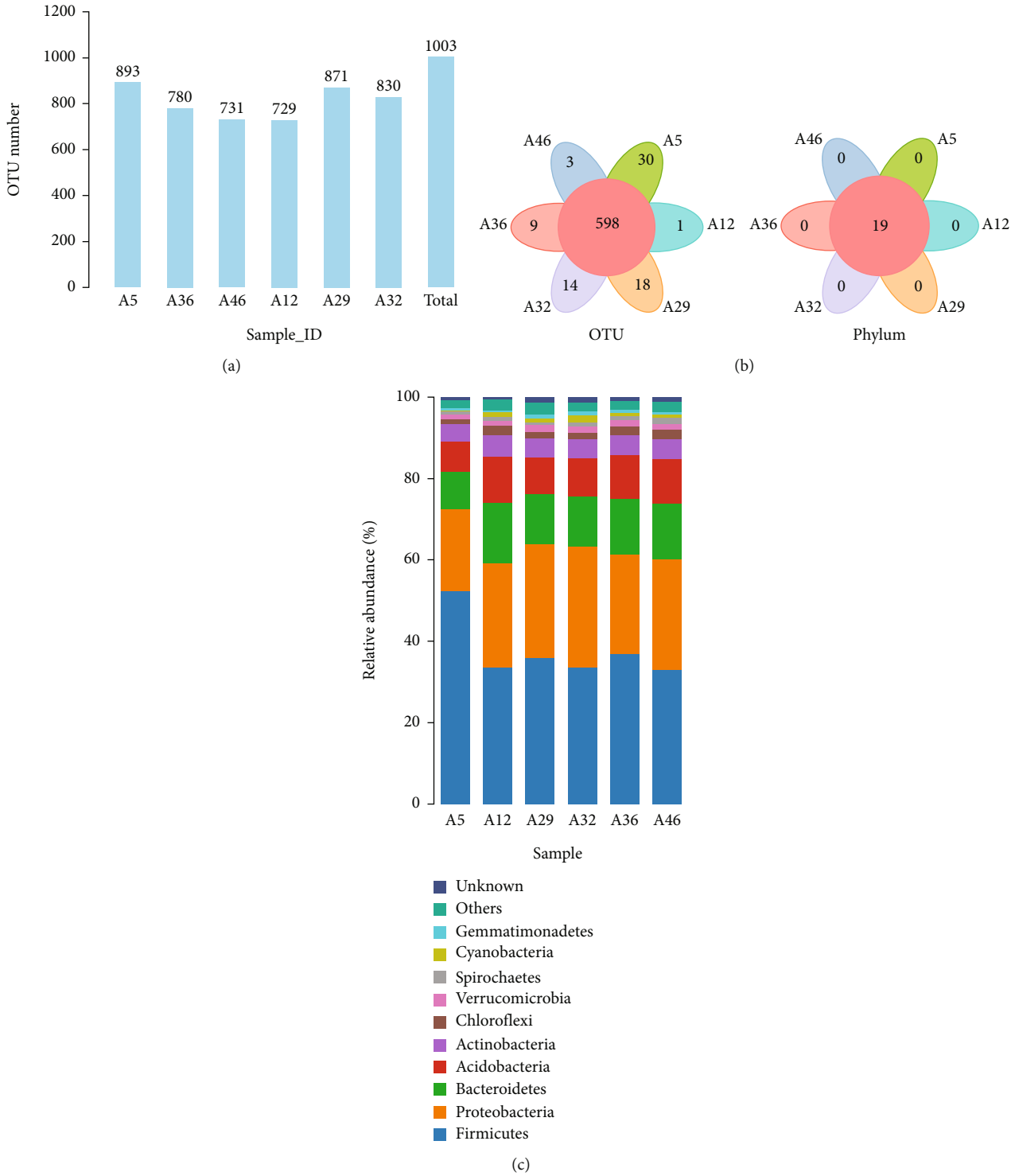

Figure 1: Continued.

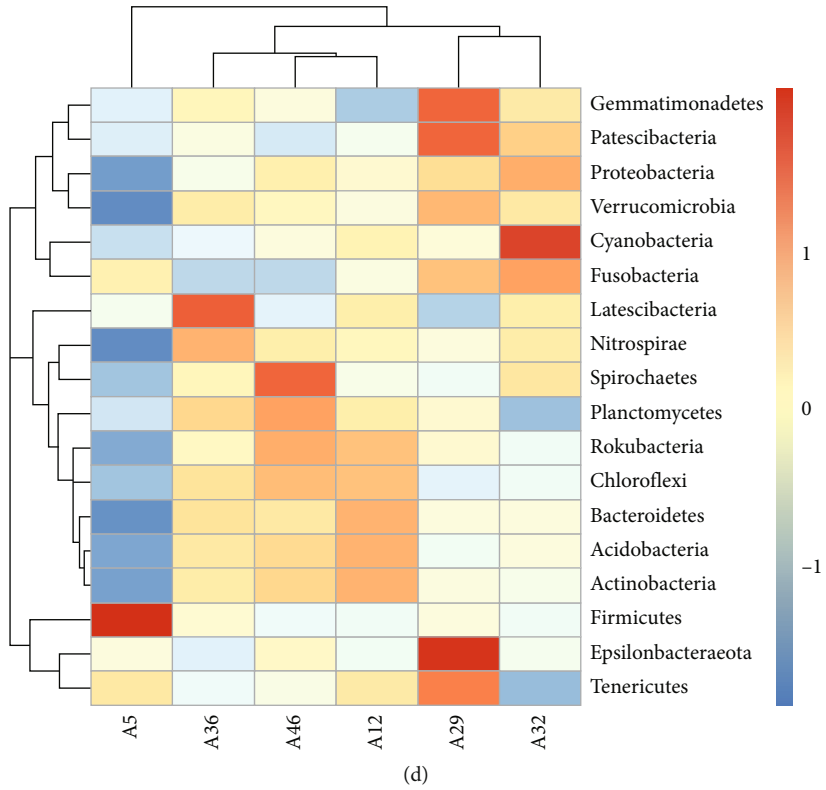

Figure 1: OTU distribution and taxonomy in liver microbiota (phyla). (a) OTU number of samples. (b) Venn diagram. (c) Species distribution (phyla). (d) Abundance heat map (phyla).

Bacteroidetes, Acidobacteria, Actinobacteria, Chloroflexi, Verrucomicrobia, Spirochaetes, Cyanobacteria, and Gemmatimonadetes were the top 10 dominant bacteria in these rats (Figure 1). CV ranged from 0.21 to 0.42 (Table S3). Microbiota annotation at the genus level is provided in Table S4.

3.2. Liver Bacteria Detected In Situ. To prove the existence and location of bacteria in the liver, we further performed histological bacteria detection *in situ*. We conducted IF using antibodies against bacterial LPS and LTA to detect Gram-negative and -positive bacteria, respectively [9]. We also used RNA FISH with a universal probe against the bacterial 16S rRNA (EUB338) to detect bacterial RNA in the liver [9]. To control for nonspecific staining, IF-negative control (no primary antibody) and FISH-negative control (nEUB338) were also applied to the samples. Bacterial LPS and 16S rRNA were positive in the liver and located in the nuclei of hepatocytes. LTA was not detected (Figure 2). We then separated the cytoplasmic and nuclear components of liver tissue and detected the expression of LPS and LTA. The results confirmed the nuclear location of LPS (Figure 3).

3.3. Functioning Analysis of the Genome Composition of Liver Microbiota. According to a Kyoto Encyclopedia of Genes and Genomes (KEGG) database comparison using the Phylogenetic Investigation of Communities by Reconstruction of Unobserved States 2 (PICRUSt2) algorithm and the tax4fun package in R, the main function composition of the genomes of annotated liver bacteria was related to metabolism ($79.92 \pm 0.24\%$). Genetic information processing ($6.31 \pm 0.10\%$), environmental information processing ($6.29 \pm 0.12\%$), and cellular processes ($3.49 \pm 0.08\%$) were less dominant and showed no obvious harm to the body ($2.58 \pm 0.06\%$). Moreover, the organismal system function ($1.41 \pm 0.02\%$) was low (Table S5).

According to BugBase analysis, liver bacteria possessed diverse phenotypes. The Gram-negative phenotype was about 1.6 times more common than the Gram-positive one, and the aerobic and anaerobic phenotypes were nearly equally common. Moreover, liver microbiota also showed high expression of mobile elements, biofilm formation, and stress tolerance as well as potentially pathogenic phenotypes (Table S6). According to faprotax analysis, the liver bacteria were mainly heterotrophic with chemoheterotrophy ($36.21 \pm 0.88\%$), fermentation ($20.33 \pm 1.61\%$), and aerobic chemoheterotrophy ($15.41 \pm 0.93\%$; Table S7) functions.

3.4. Relationship between Liver and Gut Microbiomes. The relationship between the microbiome of the liver and gut was extremely interesting. Therefore, we compared the 16S rRNA gene sequencing data of the liver microbiome with those of the fecal and ileal microbiomes. The OTU number of the liver microbiome (805.67 ± 70.14) was significantly higher than those of the SI (490.00 ± 268.20) and LI (430.50 ± 31.97), and a Chi-square of 7.520, $P < 0.05$ (Figure 4(a)). The liver microbiome shared a large percentage of bacteria with those of the ileum and feces (Figure 4(b)). At the phylum level, Proteobacteria and Acidobacteria were dominant in the liver microbiome, while the Firmicutes were lower

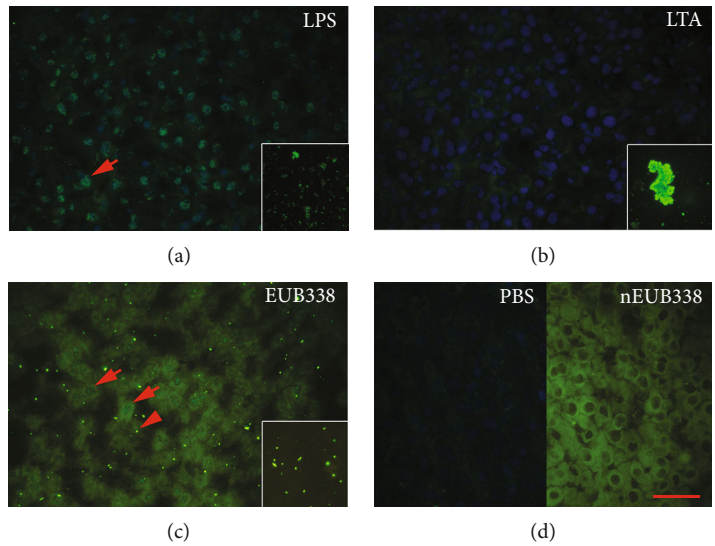

Figure 2: LPS and 16S rRNA were detected in hepatocytes. (a) LPS was detected in the nuclei of hepatocytes (arrow). Insert box: positive control of LPS with *E. coli*. (b) LTA was not detected in hepatocytes. Insert box: positive control of LTA with *Staphylococcus aureus*. (c) We detected 16S rRNA with EUB338 in the nuclei of hepatocytes (arrow). Randomly distributed bacterial contamination was the positive control (arrowhead). Insert box: positive control of 16S rRNA with *S. aureus*. (d) Negative control of IF (PBS) and FISH (nEUB338). Green, FITC labeling; blue, DAPI counterstaining. LPS: lipopolysaccharide; LTA: lipoteichoic acid. Bar = 50 μm. FITC labeling and DAPI counterstaining images were merged using the NIS-Elements D software. The exposure time was 700 ms.

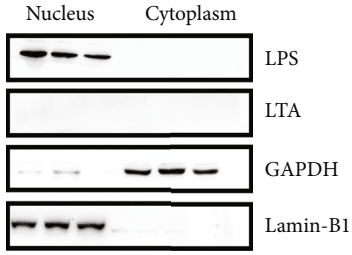

Figure 3: LPS was positive in the nuclear fraction of the liver tissues. Western blotting determined the expression patterns of the tested LPS in the rat livers. Full length gels/blots were cropped from different parts of the same gel.

than in the gut microbiome (Figure 4(c)). The heat map showed an obvious difference between the distributions of the dominant bacteria in the liver and gut microbiomes (Figure 4(d)). Except for the abundance distinction, the phylum and species distributions showed no difference (Table S8). At the genus level, among the 337 microbiota, only two bacteria (*Psychrobacter* and *Leptolyngbya VRUC 135*) were liver-exclusive, and three (*uncultured bacterium o Rhodospirillales*, *Muribacter,* and *uncultured bacterium f Rs-E47 termite group*) were exclusive to the SI and LI (Table S9), indicating remarkable homogeneity of the liver and gut microbiome.

As shown by α-diversity analysis, richness and evenness in the livers were significantly higher than in the SI or LI (Chi-square: ace 9.509, Chao1 8.187, Shannon 11.415, Simpson 10.900, $P < 0.05$; Figures 5(a) and 5(b), Table S10). According to the β-diversity analysis, the liver microbiome exhibited significantly higher similarity than the intestinal microbiome ($P < 0.05$; Figures 5(c)–5(f)). The visceral bacteria are widely considered to originate from the gut microbiome via gut leakage of the colonic mucosa (the "gut-to-liver axis"). However, the similarity of the liver microbiomes among different individuals being greater than the distance between gut and liver (Figures 5(c)–5(f)) seemed to throw this concept into doubt. We then compared the bacteria of the liver with those of the intestine. Liver bacteria showed significantly higher richness than intestinal bacteria from phylum to species level ($P < 0.05$; Table S11). We compared liver bacteria individually with gut microbiota. In each animal, a large number of liver bacteria were exclusive to the liver in comparison with the animal's ileal- and fecal-exclusive bacteria (genus level, liver: 113.67 ± 83.32 *vs.* ileum: 4.67 ± 2.58 or feces: 12.00 ± 8.15; Chi-square: 8.172; $P = 0.017$). Moreover, liver–ileum and liver–ileum–feces shared bacteria (107.67 ± 83.73 and 71.33 ± 11.78, respectively) were significantly more numerous than liver–feces shared bacteria (14.00 ± 9.44; Chi-square: 17.430; $P = 0.001$; Figure S1, Table S12). We also calculated the distance between liver and intestinal samples by the binary Jaccard method. The liver was significantly closer to the ileum than to feces (liver to liver: 0.09 ± 0.02; liver to ileum: 0.44 ± 0.25; liver to feces: 0.74 ± 0.03; $P < 0.05$; Figure 6, Table S13). These relatively independent phenomena challenged the concept of the "gut-to-liver axis," suggesting instead an upstream "liver-to-gut axis" and the possibility of bacterial translocation from the liver to the gut (Figure S2).

4. Discussion

Gut bacteria were largely overlooked until they were found to be closely related with various gut or gut-related

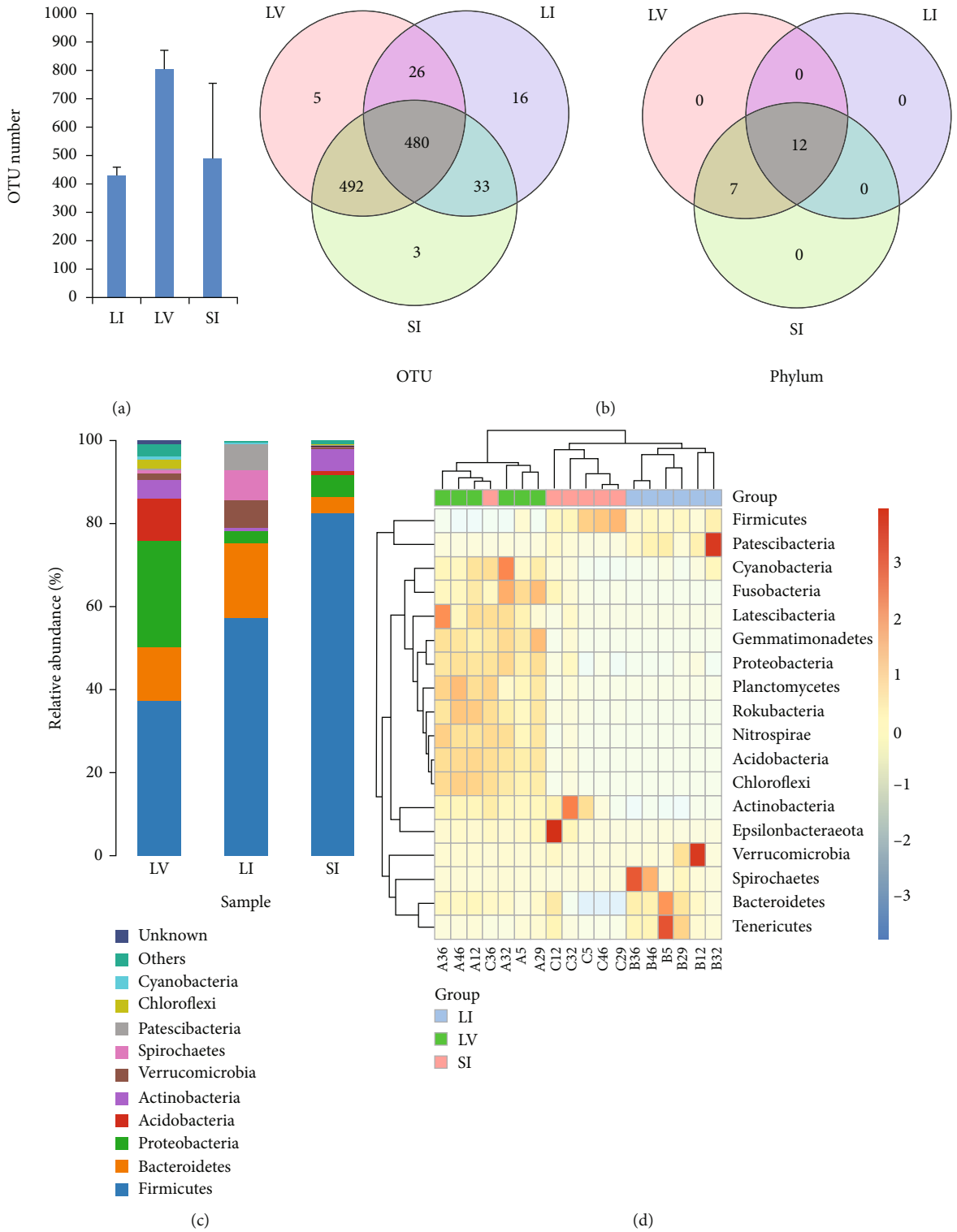

Figure 4: OTU distribution and taxonomy in the liver, ileum, and feces. (a) OTU distribution of samples. (b) Venn diagram of phyla shows shared and exclusive bacteria. (c) Species distribution (phyla). (d) Abundance heat map (phyla). Bacterial abundance: top 20; abundance ratio > 1%; distance calculation, Euclidean; cluster calculation, complete. LV: liver; LI: large intestine (feces); SI: small intestine (ileum).

disorders, such as irritable bowel syndrome [35–37], infectious diarrhea [38], ulcerative colitis, colorectal cancer, liver diseases, and obesity-related disorders [39, 40]. In addition, gut bacteria can be utilized as a medication strategy [41–45], including fecal microbiota transplantation (FMT) [46–51]. Gut bacteria recently became an explosive topic, going through roughly three development stages: (1) Feces microbiome. Findings have shown that various disorders in

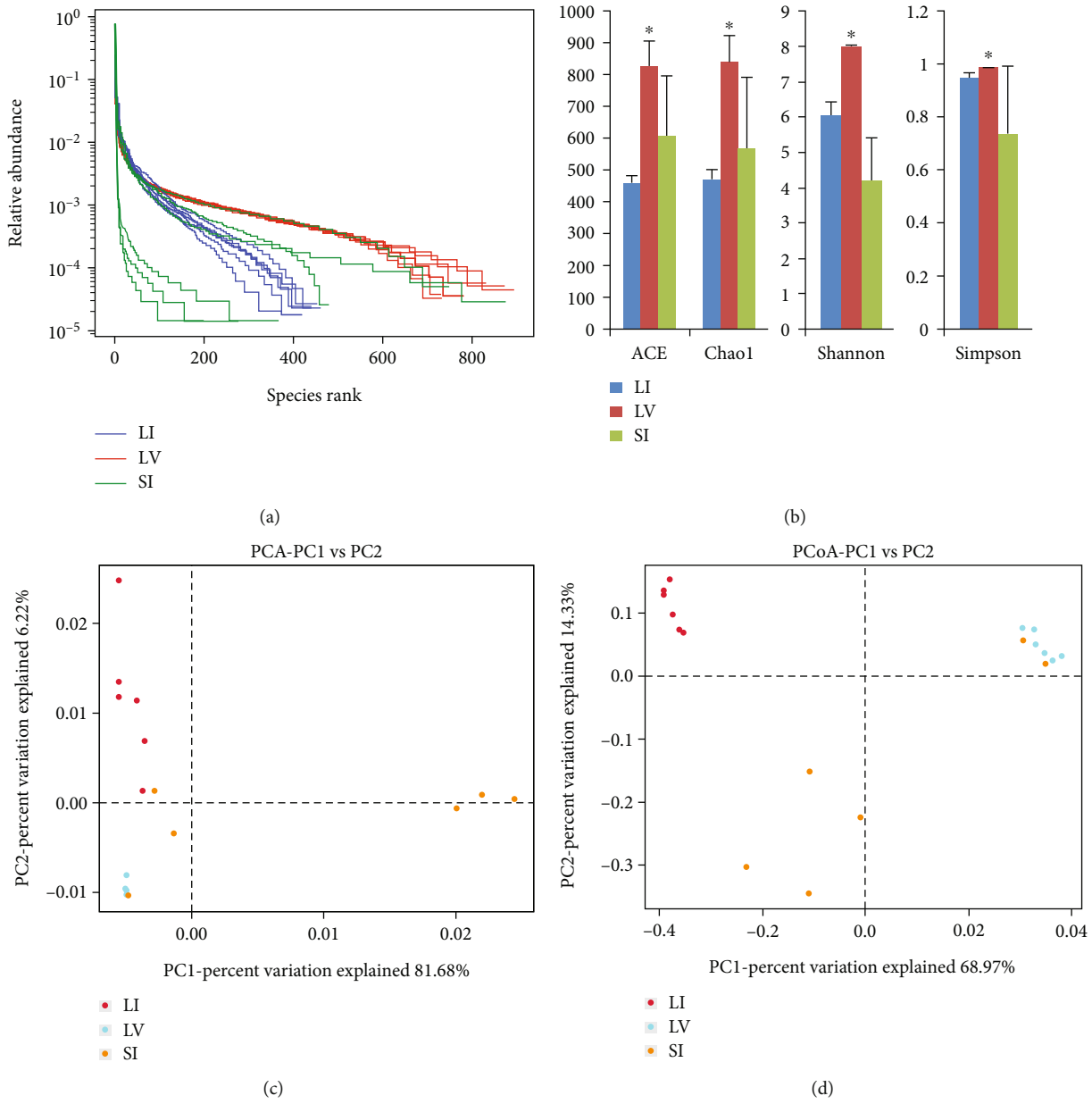

Figure 5: Continued.

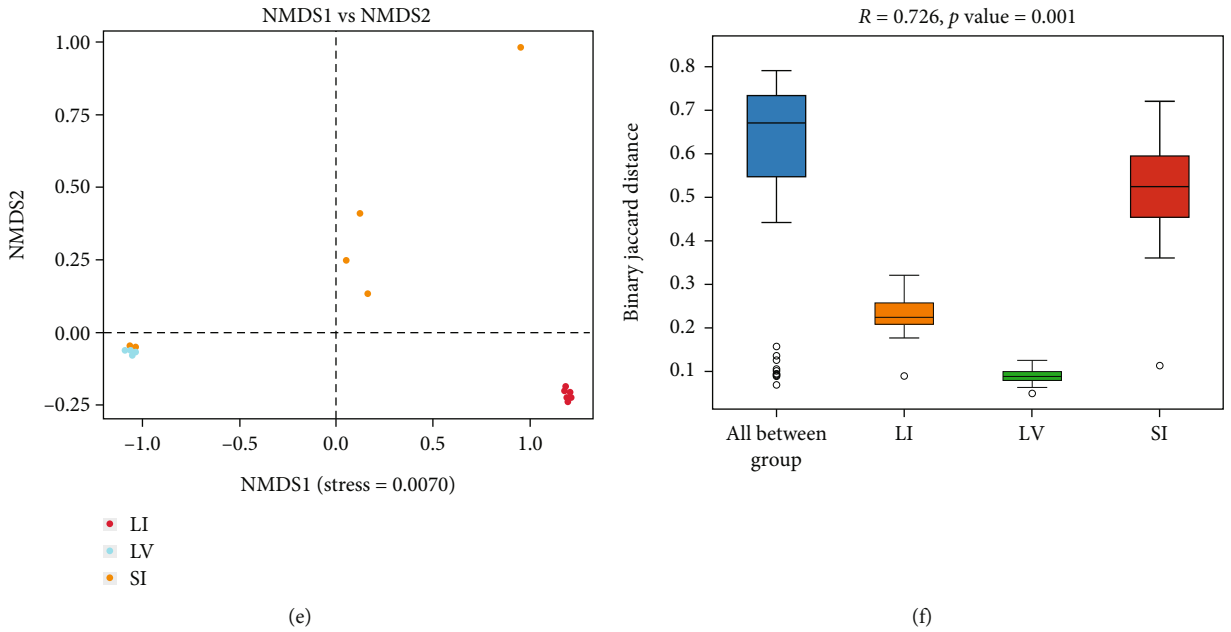

Figure 5: Alpha and beta diversity in liver and intestinal bacteria composition. Liver bacteria showed significantly higher richness and evenness than gut bacteria. The liver bacteria of different individuals were significantly more similar than the intestinal bacteria (genus level, binary Jaccard method). (a) Rank abundance curve of liver and intestinal bacteria. (b) Indices of α-diversity. $*$compared with SI and LI, $P < 0.05$. Simpson index was calculated as $1\text{-}\sum pi^2$. (c) Principal component analysis (PCA). (d) Principal coordinate analysis (PCoA). (e) Nonmetric multidimensional scaling (NMDS) analysis. (f) Analysis of similarity (ANOSIM). LV: liver; LI: large intestine (feces); SI: small intestine (ileum).

nearly every organ and system are associated with changes in the gut microbiome (samples primarily from feces) [52–68], and this has established the connection between the gut microbiome and diseases. It was suspected that gut microbiota and their metabolites, such as LPS, enter circulation (such as in bacteremia and toxemia) and result in organ injury [69, 70]. However, whether the disease-associated changes in gut microbiota occur before or after disease development cannot be determined. (2) Tissue microbiota in disease. The bacterial 16S rRNA gene as well as LPS have been detected in various tissue lesions, including tumor cells [14], leukocytes and platelet fractions [19], liver tissues of NAFLD patients [26], as well as in adipose tissues [10]. Although whether these bacteria were intact and alive remains unclear, these findings demonstrate the intimate relationship between the gut microbiome and various diseases. The key question is where these diseases arise from. The most accepted answer to this question may involve the process of gut leakage. Another question is whether they reside in the tissue before or after disease. (3) Tissue microbiota in health. Using an optimized 16S metagenomic sequencing pipeline, the bacterial 16S rRNA gene was reported in normal tissues in mice, including the brain, muscle, fat, heart, and liver [15]. This report suggested that tissue microbiota may exist in the tissue prior to the occurrence of disease.

In our study, the bacterial 16S rRNA gene was detected in the liver tissues of healthy rats. In addition, we also performed the in situ detection of EUB338, LPS, and LTA using FISH and IF, and LPS and LTA detection of nuclear and plasma extracts using western blotting. We proved that the LPS was located in the nucleus. These results strongly suggested the existence of bacteria in the liver microbiome as hidden inhabitants in the normal hepatocytes of rats. To our knowledge, in addition to the positive detection of the 16S rRNA gene, this is the first report of intracellular bacteria in normal parenchymal cells of the liver. This study switched the focus of microbiome research from the gut to the parenchymal cells. The special location and bacterial variation in the liver strongly suggested that the microbiome present in the liver was significantly different from that present in the gut. We thus named these hidden inhabitants of the liver microbiome in the normal hepatocytes of rats as the "liver microbiome."

With the help of metagenomic sequencing, we identified the existence of bacteria in the liver tissues of SD rats. We repeated the 16S rRNA gene sequencing experiment three times on two sequencing platforms (Beijing Biomarker Technologies Co., Ltd., http://www.biomarker.com.cn, Project Number: BMK191202–X098–01, BMK200916–AC763–0101, and Shanghai Bioprofile Technology Co., Ltd., Shanghai, China, http://www.bioprofile.cn, Project Number: BP20123) in ordinary or clean rats (BMK200916–AC763–0101, data not shown) and repeated the in situ detection in clean rats more than three times. All results were consistent. Because the sequencing of the 16S rRNA gene's V3–V4 region is a mature technique and a strictly controlled process, and because the technique for annotation of bacteria has been tested and widely used, these results were credible.

Bacteria in liver tissues were high in richness and abundance. A total of 1003 kinds of OTU were identified in six rats with 54,867.50 ± 6450.03 effective tags. Their α-diversity

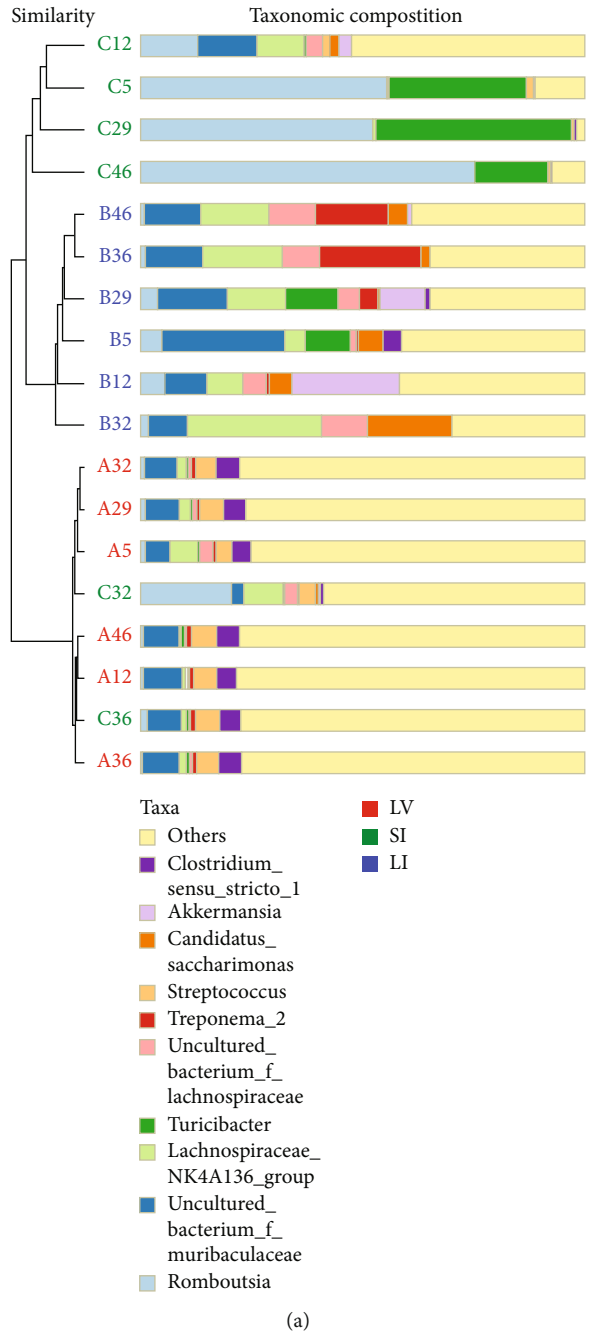

(a)

Figure 6: Continued.

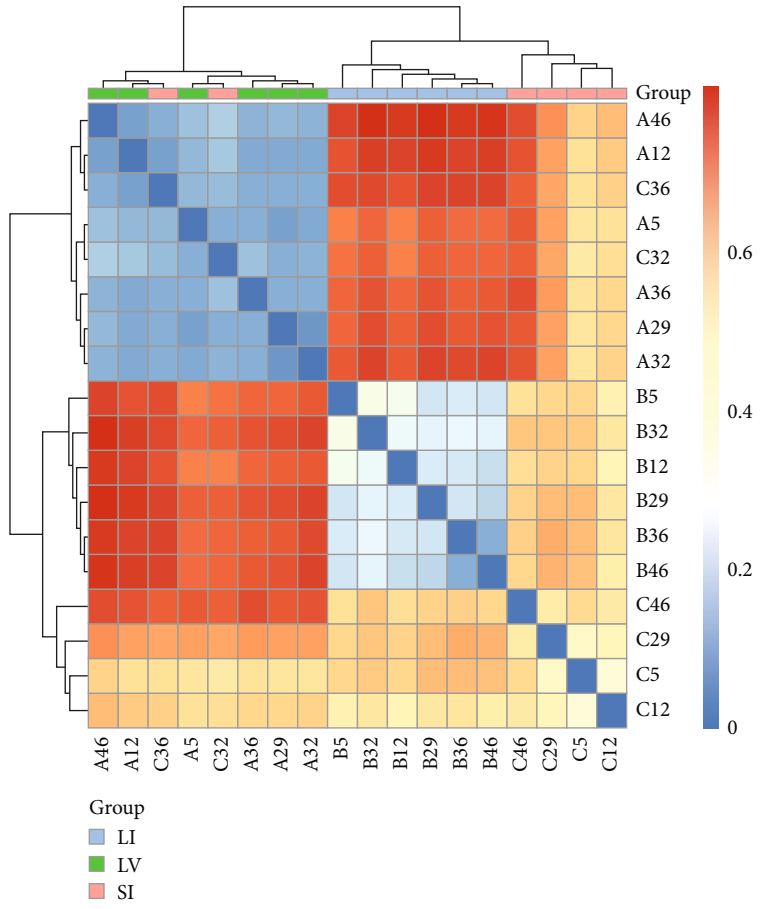

(b)

FIGURE 6: Relationship between liver and intestinal bacteria. The distance from the liver to the small intestine was smaller than that from the liver to the large intestine (genus level, binary Jaccard method). (a) Unweighted pair group method with arithmetic mean (UPGMA) analysis. (b) Distance heat map between samples. LV: liver; LI: large intestine (feces); SI: small intestine (ileum).

was even higher than that of intestinal bacteria. The most striking features of liver bacteria might be the conservation of richness, abundance, and evenness and higher similarity among different individuals compared to gut bacteria.

We further confirmed the results by LPS/LTA and EUB338 detection *in situ*. We found that bacteria were located in the nuclei of hepatocytes and were well organized. Unlike LPS and EUB338, LTA was not detectable as previously reported [26]. We hypothesized that LTA might be a less sensitive biomarker for the detection of Gram-positive bacteria in hepatocytes, or that such bacteria in hepatocytes might differ structurally from environmental Gram-positive bacteria (*e.g.*, lacking expression of LTA), because functional analysis of the genome compositions showed that the liver microbiome was highly Gram-positive and showed high percentage of chemoheterotropy, fermentation, and aerobic chemoheterotrophy. After we isolated liver tissues into the cytoplasm and nuclear components, western blotting also proved there was a strong expression of LPS in the latter, with negative in the former. LTA was not detected in both types of components.

After the identification of the liver bacterial locations, two key questions might arise: (1) where are the bacteria from, and (2) what functions do they have and by what mechanisms are they performed? The visceral bacteria have long been considered to come from the gut microbiome through the mechanism of gut leakage [13]. In this study, the liver microbiome did share bacteria with the gut microbiome, with only a few exclusive bacteria. However, in each individual, a large proportion of the liver microbiome was exclusive when compared with its gut microbiome counterpart. Moreover, in this study, the liver bacteria showed significantly higher α-diversity than the intestinal bacteria. Even if the bacteria were from the gut microbiome, how and when did they enter the liver and locate themselves in the nucleus in a well-organized manner in healthy individuals? This result challenges the gut-liver axis in which the gut is in the upstream position. One reasonable explanation is that the liver microbiota are originating from the continuing leakage of bacteria from the gut. The gut microbiota showed variation and dynamic changes caused by diet and environment [71–76], whereas the liver microbiota remained constant. Thus, this exclusivity can be acceptable to some extent. Based on the special location and difference of the gut microbiota, the liver-gut axis can be deduced, in which the liver microbiota may transport to the gut through

bile secretion [26, 77]. The gut and liver may establish a microbiota translocation circulation (Figure S2).

However, another question arises: why were the liver microbiome of different individuals significantly more similar than the gut microbiome? These findings suggest a bold hypothesis and another possibility for the origin of the liver microbiota: that the intrinsic components of the hepatocytes are inherent.

Recently, we detected the intracellular microbiota in other visceral organs of SD rats with 16S rRNA gene sequencing, and also detected the cultured cell lines HepG2, Huh-7, Hepa1-6, and HSC-T6 using the western blotting method with isolated cytoplasm and nucleus extractions as described above. Furthermore, we obtained consistent results (*Cellular Microbiota: An Inherent Inhabitant of Cells*, under review by Cellular Microbiology). However, we still need to make further efforts to design experimental plans to prove the existence and composition of the liver microbiome in human healthy liver tissues. Our results provide a profound understanding and reasonable explanation for the positive detection of intrahepatic bacteria [26, 27, 59, 77] and support the hypothesis that the liver microbiomes are inherent components of hepatocytes.

The roles of the liver microbiome are also unknown. According to the functional analysis, the functions of liver bacteria were primarily metabolic rather than those that would harm the host. This was consistent with the characteristics of native bacteria. In terms of whether these were parasitic or symbiotic, and whether these bacteria were involved in the regulation of gene expression or cell life activities, we found that the question of the origin of life may be involved. This should be further proven the way the existence of oncogenes was. Furthermore, as far as the harm to the body is concerned, are the liver bacteria associated with the development of various metabolic diseases, such as steatosis, insulin resistance, or hepatic cancer?

5. Conclusions

We found that the liver microbiome existed in hepatocytes, of which its bacterial species might be inherent inhabitants. The sources and functions (transcriptomic) of these bacteria in cell life activities and disease development should be investigated in the future.

Abbreviations

SD: Sprague Dawley
16S rRNA: 16S ribosomal ribonucleic acid
DNA: Deoxyribonucleic acid
GI: Gastrointestinal
SI: Small intestine
LI: Large intestine.

Data Availability

The raw datasets generated during the current study are available in the NCBI repository (https://www.ncbi.nlm.nih.gov/), BioProject: PRJNA820028.

Disclosure

A preprint has previously been published [78].

Conflicts of Interest

The authors declare that there are no conflicts of interest regarding the publication of this article.

Authors' Contributions

JGZ contributed to the study concept and design. XWS and JGZ contributed to the analysis and interpretation of data and drafted the manuscript. HZ completed the detection in situ. All authors contributed to the acquisition of data and critical revision of the manuscript. All authors approved the final manuscript prior to submission. XWS and HZ are shared co-first authors, and XWS and JGZ are shared co-corresponding authors.

Acknowledgments

This work was supported by the National Natural Science Foundation of China [grant number 81670776] to JGZ.

Supplementary Materials

Supplementary 1. Table S1: samples' sequencing and quality assessment. Supplementary 2. Table S2: the tags and annotated species number (in brackets) at each level. Supplementary 3. Table S3: bacteria in the liver at phylum level. Supplementary 4. Table S4: liver bacteria in rats (genus). Supplementary 5. Table S5: the main functions of liver microbiota (KEGG). Supplementary 6. Table S6: the main phenotypes of liver microbiota. Supplementary 7. Table S7: the main functions of liver microbiota. Supplementary 8. Table S8: bacteria abundance in liver and intestine of rats (phylum). Supplementary 9. Table S9: bacteria distribution in liver, small intestine, and large intestine (genus). Supplementary 10. Table S10: alpha index in liver and intestine of rats. Supplementary 11. Table S11: annotated species number in liver and intestine. Supplementary 12. Table S12: the bacteria relationship among liver, ileum, and feces of individuals. Supplementary 13. Figure S1: the bacteria distribution in the liver and intestine. Supplementary 14. Table S13: the distance between liver and intestinal samples. Supplementary 15. Figure S2: diagram of the "liver-gut" axis. Supplementary 16: Figure 2 origin images. Supplementary 17: Figure 3 full length membranes. *(Supplementary Materials)*

References

[1] E. Z. Gomaa, "Human gut microbiota/microbiome in health and diseases: a review," *Antonie Van Leeuwenhoek*, vol. 113, no. 12, pp. 2019–2040, 2020.

[2] E. Patterson, P. M. Ryan, J. F. Cryan et al., "Gut microbiota, obesity and diabetes," *Postgraduate Medical Journal*, vol. 92, no. 1087, pp. 286–300, 2016.

[3] S. Roy Sarkar and S. Banerjee, "Gut microbiota in neurodegenerative disorders," *Journal of Neuroimmunology*, vol. 328, pp. 98–104, 2019.

[4] M. Schoeler and R. Caesar, "Dietary lipids, gut microbiota and lipid metabolism," *Reviews in Endocrine & Metabolic Disorders*, vol. 20, no. 4, pp. 461–472, 2019.

[5] H. Tilg, N. Zmora, T. E. Adolph, and E. Elinav, "The intestinal microbiota fuelling metabolic inflammation," *Nature Reviews. Immunology*, vol. 20, no. 1, pp. 40–54, 2020.

[6] E. Nistal, L. E. Sáenz de Miera, M. Ballesteros Pomar et al., "An altered fecal microbiota profile in patients with non-alcoholic fatty liver disease (NAFLD) associated with obesity," *Revista Española de Enfermedades Digestivas*, vol. 111, no. 4, pp. 275–282, 2019.

[7] A. A. Kolodziejczyk, D. Zheng, O. Shibolet, and E. Elinav, "The role of the microbiome in NAFLD and NASH," *EMBO Molecular Medicine*, vol. 11, article e9302, 2019.

[8] W. M. de Vos, H. Tilg, M. Van Hul, and P. D. Cani, "Gut microbiome and health: mechanistic insights," *Gut*, vol. 71, no. 5, pp. 1020–1032, 2022.

[9] J. Amar, C. Chabo, A. Waget et al., "Intestinal mucosal adherence and translocation of commensal bacteria at the early onset of type 2 diabetes: molecular mechanisms and probiotic treatment," *EMBO Molecular Medicine*, vol. 3, no. 9, pp. 559–572, 2011.

[10] L. Massier, R. Chakaroun, S. Tabei et al., "Adipose tissue derived bacteria are associated with inflammation in obesity and type 2 diabetes," *Gut*, vol. 69, no. 10, pp. 1796–1806, 2020.

[11] R. Burcelin, M. Serino, C. Chabo et al., "Metagenome and metabolism: the tissue microbiota hypothesis," *Diabetes, Obesity & Metabolism*, vol. 15, no. s3, pp. 61–70, 2013.

[12] F. F. Anhê, B. A. H. Jensen, T. V. Varin et al., "Type 2 diabetes influences bacterial tissue compartmentalisation in human obesity," *Nature Metabolism*, vol. 2, no. 3, pp. 233–242, 2020.

[13] M. Camilleri and A. Vella, "What to do about the leaky gut," *Gut*, vol. 71, no. 2, pp. 424–435, 2022.

[14] D. Nejman, I. Livyatan, G. Fuks et al., "The human tumor microbiome is composed of tumor type-specific intracellular bacteria," *Science*, vol. 368, no. 6494, pp. 973–980, 2020.

[15] J. Lluch, F. Servant, S. Païssé et al., "The characterization of novel tissue microbiota using an optimized 16S metagenomic sequencing pipeline," *PLoS One*, vol. 10, no. 11, article e0142334, 2015.

[16] C. M. Dunn, C. Velasco, A. Rivas et al., "Identification of cartilage microbial DNA signatures and associations with knee and hip osteoarthritis," *Arthritis & Rhematology*, vol. 72, no. 7, pp. 1111–1122, 2020.

[17] J. M. Berthelot, F. Lioté, and J. Sibilia, "Tissue microbiota: A 'secondary-self', first target of autoimmunity?," *Joint Bone Spine*, vol. 89, no. 2, article 105337, 2022.

[18] L. Hosang, R. C. Canals, F. J. van der Flier et al., "The lung microbiome regulates brain autoimmunity," *Nature*, vol. 603, no. 7899, pp. 138–144, 2022.

[19] S. Païssé, C. Valle, F. Servant et al., "Comprehensive description of blood microbiome from healthy donors assessed by 16S targeted metagenomic sequencing," *Transfusion*, vol. 56, no. 5, pp. 1138–1147, 2016.

[20] D. C. Emery, T. L. Cerajewska, J. Seong et al., "Comparison of blood bacterial communities in periodontal health and periodontal disease," *Frontiers in Cellular and Infection Microbiology*, vol. 10, article 577485, 2021.

[21] E. Whittle, M. O. Leonard, R. Harrison, T. W. Gant, and D. P. Tonge, "Multi-method characterization of the human circulating microbiome," *Frontiers in Microbiology*, vol. 9, p. 3266, 2019.

[22] S. J. Jeon, F. Cunha, A. Vieira-Neto et al., "Blood as a route of transmission of uterine pathogens from the gut to the uterus in cows," *Microbiome*, vol. 5, no. 1, p. 109, 2017.

[23] A. I. Vientós-Plotts, A. C. Ericsson, H. Rindt et al., "Dynamic changes of the respiratory microbiota and its relationship to fecal and blood microbiota in healthy young cats," *PLoS One*, vol. 12, no. 3, article e0173818, 2017.

[24] R. K. Mandal, T. Jiang, A. A. Al-Rubaye et al., "An investigation into blood microbiota and its potential association with bacterial Chondronecrosis with osteomyelitis (BCO) in broilers," *Scientific Reports*, vol. 6, no. 1, article 25882, 2016.

[25] R. Cianci, L. Franza, M. G. Massaro et al., "The crosstalk between gut microbiota, intestinal immunological niche and visceral adipose tissue as a new model for the pathogenesis of metabolic and inflammatory diseases: the paradigm of type 2 diabetes mellitus," *Current Medicinal Chemistry*, vol. 29, no. 18, pp. 3189–3201, 2022.

[26] S. Sookoian, A. Salatino, G. O. Castaño et al., "Intrahepatic bacterial metataxonomic signature in non-alcoholic fatty liver disease," *Gut*, vol. 69, no. 8, pp. 1483–1491, 2020.

[27] H. Tilg, R. Burcelin, and V. Tremaroli, "Liver tissue microbiome in NAFLD: next step in understanding the gut-liver axis?," *Gut*, vol. 69, no. 8, pp. 1373-1374, 2020.

[28] K. Chen, X. Luan, Q. Liu et al., "_Drosophila_ Histone Demethylase KDM5 Regulates Social Behavior through Immune Control and Gut Microbiota Maintenance," *Cell Host & Microbe*, vol. 25, no. 4, pp. 537–552.e8, 2019.

[29] C. Yang, Z. Xu, Q. Deng, Q. Huang, X. Wang, and F. Huang, "Beneficial effects of flaxseed polysaccharides on metabolic syndrome via gut microbiota in high-fat diet fed mice," *Food Research International*, vol. 131, article 108994, 2020.

[30] A. M. Bolger, M. Lohse, and B. Usadel, "Trimmomatic: a flexible trimmer for Illumina sequence data," *Bioinformatics*, vol. 30, no. 15, pp. 2114–2120, 2014.

[31] R. C. Edgar, B. J. Haas, J. C. Clemente, C. Quince, and R. Knight, "UCHIME improves sensitivity and speed of chimera detection," *Bioinformatics*, vol. 27, no. 16, pp. 2194–2200, 2011.

[32] R. C. Edgar, "UPARSE: highly accurate OTU sequences from microbial amplicon reads," *Nature Methods*, vol. 10, no. 10, pp. 996–998, 2013.

[33] C. Quast, E. Pruesse, P. Yilmaz et al., "The SILVA ribosomal RNA gene database project: improved data processing and web-based tools," *Nucleic Acids Research*, vol. 41, pp. D590–D596, 2013.

[34] Q. Wang, G. M. Garrity, J. M. Tiedje, and J. R. Cole, "Naive Bayesian classifier for rapid assignment of rRNA sequences into the new bacterial taxonomy," *Applied and Environmental Microbiology*, vol. 73, no. 16, pp. 5261–5267, 2007.

[35] G. Dahlqvist and H. Piessevaux, "Irritable bowel syndrome: the role of the intestinal microbiota, pathogenesis and therapeutic targets," *Acta Gastroenterologica Belgica*, vol. 74, pp. 375–380, 2011.

[36] E. M. Quigley, "Bacterial flora in irritable bowel syndrome: role in pathophysiology, implications for management," *Journal of Digestive Diseases*, vol. 8, no. 1, pp. 2–7, 2007.

[37] K. L. Glassner, B. P. Abraham, and E. M. M. Quigley, "The microbiome and inflammatory bowel disease," *The Journal of*

Allergy and Clinical Immunology, vol. 145, no. 1, pp. 16–27, 2020.

[38] C. M. Surawicz, "Le microbiote dans les diarrhées infectieuses [the microbiota and infectious diarrhea]," *Gastroentérologie Clinique et Biologique*, vol. 34, Supplement 1, pp. 31–40, 2010.

[39] J. R. Marchesi, D. H. Adams, F. Fava et al., "The gut microbiota and host health: a new clinical frontier," *Gut*, vol. 65, no. 2, pp. 330–339, 2016.

[40] A. J. Czaja, "Factoring the intestinal microbiome into the pathogenesis of autoimmune hepatitis," *World Journal of Gastroenterology*, vol. 22, no. 42, pp. 9257–9278, 2016.

[41] K. P. Lemon, G. C. Armitage, D. A. Relman, and M. A. Fischbach, "Microbiota-targeted therapies: an ecological perspective," *Science Translational Medicine*, vol. 4, no. 137, 2012.

[42] M. Elahi, H. Nakayama-Imaohji, M. Hashimoto et al., "The human gut microbe *bacteroides thetaiotaomicron* suppresses toxin release from *clostridium difficile* by inhibiting autolysis," *Antibiotics*, vol. 10, no. 2, p. 187, 2021.

[43] A. Rehman, F. A. Heinsen, M. E. Koenen et al., "Effects of probiotics and antibiotics on the intestinal homeostasis in a computer controlled model of the large intestine," *BMC Microbiology*, vol. 12, no. 1, p. 47, 2012.

[44] I. Ekmekciu, E. von Klitzing, U. Fiebiger et al., "The probiotic compound VSL#3 modulates mucosal, peripheral, and systemic immunity following murine broad-spectrum antibiotic treatment," *Frontiers in Cellular and Infection Microbiology*, vol. 7, p. 167, 2017.

[45] B. Yousefi, M. Eslami, A. Ghasemian, P. Kokhaei, A. Salek Farrokhi, and N. Darabi, "Probiotics importance and their immunomodulatory properties," *Journal of Cellular Physiology*, vol. 234, no. 6, pp. 8008–8018, 2019.

[46] E. van Nood, A. Vrieze, M. Nieuwdorp et al., "Duodenal infusion of donor feces for recurrent Clostridium difficile," *The New England Journal of Medicine*, vol. 368, no. 5, pp. 407–415, 2013.

[47] C. P. Kelly, "Fecal microbiota transplantation–an old therapy comes of age," *The New England Journal of Medicine*, vol. 368, no. 5, pp. 474-475, 2013.

[48] C. Barba, C. O. Soulage, G. Caggiano, G. Glorieux, D. Fouque, and L. Koppe, "Effects of fecal microbiota transplantation on composition in mice with CKD," *Toxins*, vol. 12, no. 12, p. 741, 2020.

[49] S. M. Vindigni and C. M. Surawicz, "Fecal microbiota transplantation," *Gastroenterology Clinics of North America*, vol. 46, no. 1, pp. 171–185, 2017.

[50] A. Alharthi, S. Alhazmi, N. Alburae, and A. Bahieldin, "The human gut microbiome as a potential factor in autism spectrum disorder," *International Journal of Molecular Sciences*, vol. 23, no. 3, p. 1363, 2022.

[51] I. Ekmekciu, E. von Klitzing, C. Neumann et al., "Fecal microbiota transplantation, commensal *Escherichia coli* and *lactobacillus johnsonii* strains differentially restore intestinal and systemic adaptive immune cell populations following broad-spectrum antibiotic treatment," *Frontiers in Microbiology*, vol. 8, p. 2430, 2017.

[52] L. H. Morais, H. L. Schreiber 4th, and S. K. Mazmanian, "The gut microbiota-brain axis in behaviour and brain disorders," *Nature Reviews Microbiology*, vol. 19, no. 4, pp. 241–255, 2021.

[53] E. M. M. Quigley, "Microbiota-brain-gut axis and neurodegenerative diseases," *Current Neurology and Neuroscience Reports*, vol. 17, no. 12, p. 94, 2017.

[54] S. Mörkl, M. I. Butler, A. Holl, J. F. Cryan, and T. G. Dinan, "Probiotics and the microbiota-gut-brain axis: focus on psychiatry," *Current Nutrition Reports*, vol. 9, no. 3, pp. 171–182, 2020.

[55] A. Megur, D. Baltriukienė, V. Bukelskienė, and A. Burokas, "The microbiota–gut–brain axis and alzheimer's disease: neuroinflammation is to blame?," *Nutrients*, vol. 13, p. 37, 2021.

[56] T. G. Dinan and J. F. Cryan, "Brain-gut-microbiota axis and mental health," *Psychosomatic Medicine*, vol. 79, no. 8, pp. 920–926, 2017.

[57] M. Witkowski, T. L. Weeks, and S. L. Hazen, "Gut microbiota and cardiovascular disease," *Circulation Research*, vol. 127, no. 4, pp. 553–570, 2020.

[58] F. Z. Marques, E. Nelson, P. Y. Chu et al., "High-fiber diet and acetate supplementation change the gut microbiota and prevent the development of hypertension and heart failure in hypertensive mice," *Circulation*, vol. 135, no. 10, pp. 964–977, 2017.

[59] R. Wang, R. Tang, B. Li, X. Ma, B. Schnabl, and H. Tilg, "Gut microbiome, liver immunology, and liver diseases," *Cellular & Molecular Immunology*, vol. 18, no. 1, pp. 4–17, 2021.

[60] K. F. Budden, S. L. Gellatly, D. L. Wood et al., "Emerging pathogenic links between microbiota and the gut-lung axis," *Nature Reviews. Microbiology*, vol. 15, no. 1, pp. 55–63, 2017.

[61] A. Dumas, L. Bernard, Y. Poquet, G. Lugo-Villarino, and O. Neyrolles, "The role of the lung microbiota and the gut–lung axis in respiratory infectious diseases," *Cellular Microbiology*, vol. 20, no. 12, article e12966, 2018.

[62] G. P. Hobby, O. Karaduta, G. F. Dusio, M. Singh, B. L. Zybailov, and J. M. Arthur, "Chronic kidney disease and the gut microbiome," *American Journal of Physiology Renal Physiology*, vol. 316, no. 6, pp. F1211–F1217, 2019.

[63] C. O. Iatcu, A. Steen, and M. Covasa, "Gut microbiota and complications of type-2 diabetes," *Nutrients*, vol. 14, no. 1, p. 166, 2022.

[64] C. Antza, S. Stabouli, and V. Kotsis, "Gut microbiota in kidney disease and hypertension," *Pharmacological Research*, vol. 130, pp. 198–203, 2018.

[65] P. D'Amelio and F. Sassi, "Gut microbiota, immune system, and bone," *Calcified Tissue International*, vol. 102, no. 4, pp. 415–425, 2018.

[66] D. Quach and R. A. Britton, "Gut microbiota and bone health," *Advances in Experimental Medicine and Biology*, vol. 1033, pp. 47–58, 2017.

[67] C. Y. L. Chong, F. H. Bloomfield, and J. M. O'Sullivan, "Factors affecting gastrointestinal microbiome development in neonates," *Nutrients*, vol. 10, no. 3, p. 274, 2018.

[68] D. D. Nyangahu and H. B. Jaspan, "Influence of maternal microbiota during pregnancy on infant immunity," *Clinical and Experimental Immunology*, vol. 198, no. 1, pp. 47–56, 2019.

[69] L. K. Ursell, H. J. Haiser, W. Van Treuren et al., "The intestinal metabolome: an intersection between microbiota and host," *Gastroenterology*, vol. 146, no. 6, pp. 1470–1476, 2014.

[70] Y. Dong, Y. Yuan, Y. Ma et al., "Combined intestinal metabolomics and microbiota analysis for acute endometritis induced by lipopolysaccharide in mice," *Frontiers in Cellular and Infection Microbiology*, vol. 11, article 791373, 2021.

[71] L. G. Albenberg and G. D. Wu, "Diet and the intestinal microbiome: associations, functions, and implications for health and

disease," *Gastroenterology*, vol. 146, no. 6, pp. 1564–1572, 2014.

[72] N. Zmora, J. Suez, and E. Elinav, "You are what you eat: diet, health and the gut microbiota," *Nature Reviews Gastroenterology & Hepatology*, vol. 16, no. 1, pp. 35–56, 2019.

[73] R. K. Weersma, A. Zhernakova, and J. Fu, "Interaction between drugs and the gut microbiome," *Gut*, vol. 69, no. 8, pp. 1510–1519, 2020.

[74] S. Bibbò, G. Ianiro, V. Giorgio et al., "The role of diet on gut microbiota composition," *European Review for Medical and Pharmacological Sciences*, vol. 20, no. 22, pp. 4742–4749, 2016.

[75] M. Song and A. T. Chan, "Environmental factors, gut microbiota, and colorectal cancer prevention," *Clinical Gastroenterology and Hepatology*, vol. 17, no. 2, pp. 275–289, 2019.

[76] B. Strasser, M. Wolters, C. Weyh, K. Krüger, and A. Ticinesi, "The effects of lifestyle and diet on gut microbiota composition, inflammation and muscle performance in our aging society," *Nutrients*, vol. 13, no. 6, p. 2045, 2021.

[77] N. Grüner and J. Mattner, "Bile acids and microbiota: multifaceted and versatile regulators of the liver-gut axis," *International Journal of Molecular Sciences*, vol. 22, no. 3, p. 1397, 2021.

[78] https://www.researchsquare.com/article/rs-1352724/v1.